J. Fluid Mech. (1993), *vol.* 250, *pp.* 609–633

Experimental studies of the deformation and breakup of a synthetic capsule in steady and unsteady simple shear flow

By K. S. CHANG† AND W. L. OLBRICHT
School of Chemical Engineering, Cornell University, Ithaca, NY 14853, USA

(Received 20 February 1992 and in revised form 19 October 1992)

An experimental study is reported of the motion, deformation, and breakup of a synthetic capsule that is freely suspended in Couette flow. The capsule is a liquid drop surrounded by a thin polymeric membrane. The shape and orientation of the capsule are measured in steady flow and following the start-up of Couette flow. Results are compared with predictions of the small-deformation theory of Barthes-Biesel and co-workers. The data suggest that the capsule membrane is viscoelastic, and comparisons with theory yield values of the membrane elastic modulus and the membrane viscosity. The values of the elastic modulus of the capsule membrane deduced from the flow data are compared with independent measurements for the same capsule.

When the flow-induced deformation becomes sufficiently large, the capsules break. Breakup begins at points on the membrane surface near the principal strain axis of the undisturbed flow. By examining the local deformation within the membrane, it is shown that breakup is correlated with local thinning of the membrane and is initiated at points where the thickness is a minimum.

1. Introduction

This paper describes observations of the deformation and breakup of synthetic, liquid-filled capsules in an approximate simple shear flow generated in a Couette device. Capsules are composite particles consisting of a viscous inner fluid surrounded by a thin membrane. In the accompanying paper, Chang & Olbricht (1993) describe a method of formulating macroscopic capsules that can be used to study the flow-induced deformation of the capsules in a manner similar to previous investigations of the deformation of liquid drops. It was shown that measurements of the shape of the capsule in hyperbolic extensional flow agreed reasonably well with results of the small-deformation theory developed by Barthes-Biesel and co-workers for a thin, linear viscoelastic membrane, provided the deformation was not too large. In steady hyperbolic extension, the deformation of the capsule for a given strain rate is limited by the elastic modulus of the capsule membrane. The results of the small-deformation theory were used to deduce the elastic modulus of the capsule membrane from the measurements of capsule deformation as a function of strain rate. The resulting values of the elastic modulus were compared with values measured for each capsule using a different method, viz. the deformation of the capsule between parallel plates under a known load. Reasonable agreement between the two methods was found, thus further corroborating the predictions of theory and suggesting that the viscoelastic constitutive properties of a capsule membrane can be probed by deforming the capsules in flow.

† Present address: Kimberly-Clark, 2100 Winchester Road, Neenah, WI 54957-0999, USA.

For steady hyperbolic extension, the capsule shape depends neither on the viscosity of the fluid inside the capsule nor on the viscous behaviour of the membrane itself, because the flow does not permit any motion of the membrane that could generate a flow inside the drop. However, the shape of a capsule in steady simple shear flow depends not only on the elastic response of the membrane but also on its viscous response, even when the shape of the capsule is steady in time. The membrane viscosity affects the steady-state shape because the membrane rotates or 'tank-treads' in simple shear flow. Every piece of the membrane undergoes an unsteady deformation in a Lagrangian sense as the membrane rotates about the inner contents of the capsule. Thus, the membrane can dissipate energy even though its overall shape does not change. The rate of energy dissipation depends on the membrane viscosity. In this case the constitutive behaviour of the linear viscoelastic membrane can be described in terms of two parameters, a Hookean elastic modulus Eh and a viscous modulus μ^s. The shape of such a capsule freely suspended in simple shear flow has been solved in the limit of small deformations by Barthes-Biesel & Sgaier (1985). As far as we are aware, the only tests of this theory are based on comparisons of rheological data for capsule suspensions with theoretical predictions derived from the small-deformation results.

This paper describes experiments to test directly the predictions of the small-deformation theory and to identify the range of parameters over which the theory holds by observation of synthetic capsules in simple shear flow. We also seek to determine whether measurements of the deformation and orientation of a capsule in simple shear flow can be used to deduce simultaneously values of the membrane constitutive parameters, in this case both Eh and μ^s. Furthermore, we examine the nonlinear rheological behaviour of the capsule membrane in simple shear flow and compare with results obtained in extensional flow for deformations outside the limits of the theory. For the case of simple shear, we examine the response of capsules for deformations that are sufficiently large to cause capsule breakup.

The response of the capsules in this experiment bears a qualitative resemblance to the motion and deformation of red blood cells in simple shear flow, although there are important differences. Individual red blood cells have been examined in simple shear and Poiseuille flow by several investigators (e.g. Schmid-Schönbein & Wells 1969 and Goldsmith & Marlow 1972). For relatively small shear rates, the cells are hardly deformed from their rest shape, which is a biconcave disk, and they exhibit a periodic flipping motion that is reminiscent of the motion of rigid ellipsoids in simple shear flow. However, for sufficiently high shear rates the cells deform and exhibit steady shapes with a fixed orientation with respect to the streamlines of the undisturbed flow, while the membrane circulates about the interior of the membrane. Keller & Skalak (1982) developed a model that shows how the transition from the flipping motion to the steady shape depends on the shape of the particle and on the ratio of interior fluid viscosity to exterior fluid viscosity.

The experiments described in this report involve only macroscopic capsules examined individually, so that the properties of a capsule deduced from the flow experiment can be compared with measurements employing independent methods. Most capsules that are used in technologically important applications or that occur naturally in biological systems are micoscopic or sub-microscopic in size. Nevertheless, we expect that if a dilute suspension of microscopic capsules were examined in flow using some optical method such as dichroism or birefringence, the membrane properties of the capsules could be deduced from some measure of average particle shape, provided the predicted relationships between material properties and response in flow can be understood for simpler systems.

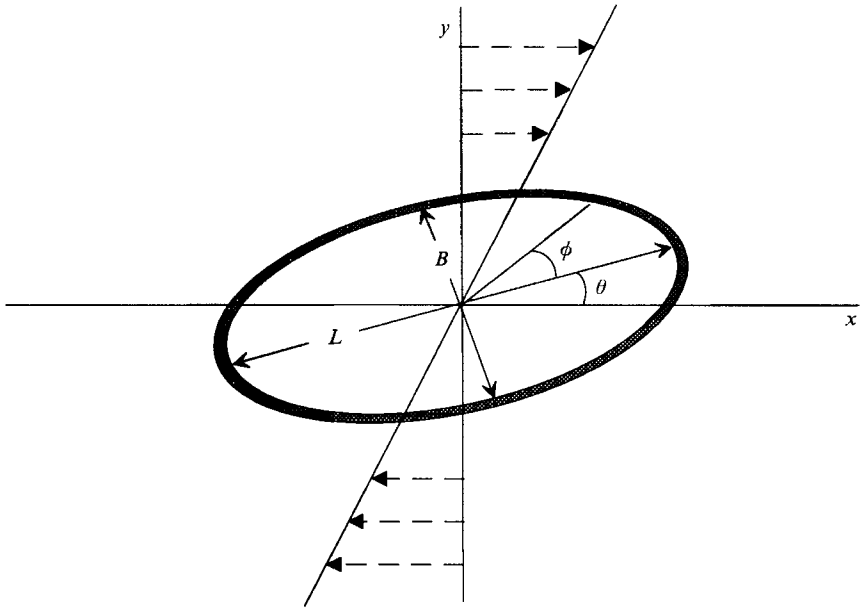

FIGURE 1. Schematic of a capsule in simple shear flow defined by $v_x = Gy$. The major axis of the capsule is specified by the angle θ. The angle ϕ is used to specify points on the capsule surface in the (x, y)-plane.

2. Experimental

Figure 1 shows a schematic of a deformed capsule in simple shear flow defined by $v_x = Gy$. The capsule interior is a Newtonian liquid of viscosity $\lambda\mu$, and the capsule is suspended in a Newtonian liquid of viscosity μ. The thickness of the capsule membrane is h, which is small compared with the undeformed capsule radius a. Provided the deformation is not too large, a parameter that describes the shape of the capsule is the Taylor deformation parameter $D_{12} = (L-B)/(L+B)$, where L and B are the major and minor axes of the capsule, respectively. The principal axes of the deformed capsule are in the (x, y)-plane defined as $z = 0$, which also contains the centre of mass of the capsule. The orientation of the capsule is specified by the angle θ, which is measured counterclockwise from the positive x-axis. The angle ϕ, which is drawn counterclockwise from the major axis of the capsule, will be used to identify points on the capsule surface in the $z = 0$ plane.

Our studies of capsule motion are carried out in a Couette cell consisting of two counter-rotating concentric cylinders, as illustrated in figure 2. The outer cylinder, which is made of Pyrex, has an inner diameter of 28.893 ± 0.064 cm. The inner cylinder, which is made of copper, has an outer diameter of 17.780 ± 0.003 cm. The height of the cylinders is 25.4 cm.

Each cylinder is rotated by a DC stepping motor (Compumotor PK2-83-62) that is connected to the cylinder drive shaft by interchangeable couplers and gear reducers. The stepping rates of the motors are controlled by an indexer card (Compumotor PC-23), which is housed in an IBM PC. The signal driving the stepping motor is sent from the indexer card to a PC23 Adaptor (Compumotor), which then sends a 10 μs pulse to a Type PK2 (Compumotor) stepping motor drive.

The motor that drives the outer cylinder is mounted directly below the Couette cell, and the motor that drives the inner cylinder is mounted above the Couette cell. The two cylinder/drive systems are completely independent; the weight of the outer cylinder

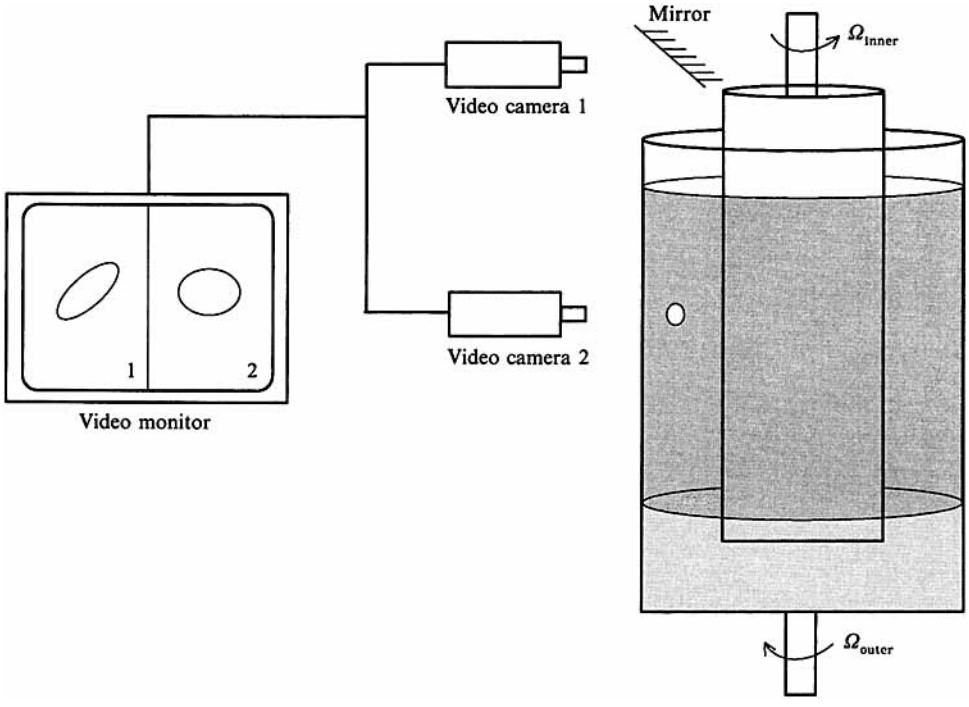

FIGURE 2. Schematic of the Couette apparatus.

and the working fluid is supported by a thrust bearing (FAG 51160M), while the inner cylinder is freely suspended from its drive shaft. The error in the alignment of the two drive shafts is much smaller than the variations in the diameters of the two cylinders.

The motors operate with a resolution of 200 full steps or 400 half-steps per revolution. Both drive systems contain in-line 48.75:1 gear reducers. With the motors operating in the half-step mode, the range of shear rates that can be obtained is 0.05 to 45 s^{-1}. To expand the range of shear rates that can be covered, the cylinders can be replaced with cylinders of different sizes, and the couplings to the stepper motors and gear reducers can be replaced without dismantling the apparatus.

The space between the cylinders is filled with polybutene, which has a specific gravity very close to that of the capsules. The viscosity of polybutene at room temperature is about 100 P, which ensures that the Reynolds number based on the capsule diameter is smaller than 0.03 for all experimental conditions. Similarly, the maximum value of the Taylor number is 0.6, which means that secondary flows associated with the Taylor instability are not important.

To eliminate end effects caused by the bottom of the Couette cell, a thin layer of water, which is immiscible with polybutene, is placed on the bottom of the cell. The top of the Couette cell is open to the atmosphere. There is no evidence of disturbances in the flow due to end effects except in regions very close to the top and bottom interfaces. The capsule is never allowed to enter these regions during an experiment.

The shear rate in the gap between the cylinders varies with radial position owing to the curvatures of the cylinders. The variation in shear rate ΔG_r over a length comparable to the diameter of a capsule is estimated as:

$$\frac{\Delta G_r}{G_r} = r^2\left(\frac{1}{(r-a)^2} - \frac{1}{(r+a)^2}\right), \tag{1}$$

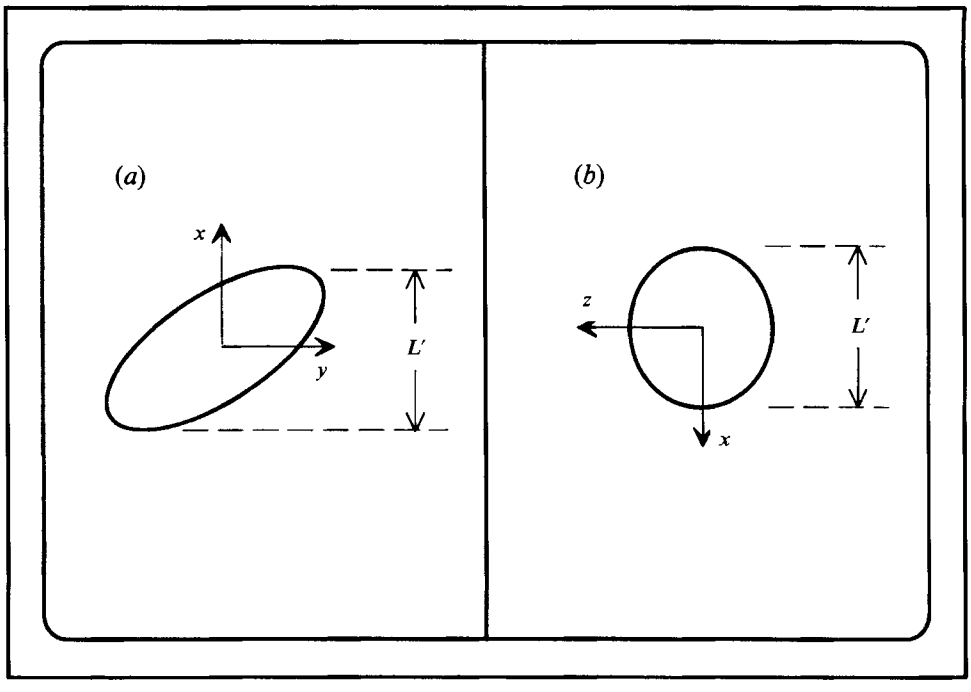

FIGURE 3. Schematic of the video monitor display showing two orthogonal views of the capsule in simple shear flow defined by $v_x = Gy$: (*a*) top view, i.e. the projection of the capsule surface onto the (x, y)-plane; (*b*) side view, i.e. the projection of the capsule surface onto the (x, z)-plane.

where G_r is the shear rate for a capsule whose centre is located at radial coordinate r, and a is the undeformed capsule radius. The maximum fractional variation in the shear rate $\Delta G_r/G_r$ across the capsule is 0.08. Small variations in the diameters of the cylinders introduce additional variations in the shear rate, but the maximum value of $\Delta G_r/G_r$ due to this effect is 0.0054, which is much smaller than the variation in shear rate due to cylinder curvature.

After a capsule is placed in the region between the cylinders and the flow is started, the motion and deformation of the capsule are recorded continuously by CCD video cameras (Panasonic BD404). The video cameras are synchronized with a strobe light system (Display Integration Technology) to improve the resolution of the recorded images. One of the video cameras is mounted above the Couette cell to photograph the projection of the capsule shape in the shear plane; the other camera is mounted outside the outer cylinder to provide an orthogonal projection of the capsule shape.

The video signals from the two cameras are displayed simultaneously using an image splitter (Burle) and a high-resolution variscan monitor (Electrohome EVM-2319). The video monitor display is shown schematically in figure 3. The image on the left is a top view of the capsule, i.e. the projection of the capsule surface onto the (x, y)-plane, cf. figure 1. The image on the right is taken by a camera aimed in the negative y-direction, which gives the projection of the capsule surface onto the (x, z)-plane. Because of the way the camera is mounted, the image on the left is rotated 90°, and it is inverted by passing through the mirror shown in figure 2. The orientations of the x-, y-, and z-axes defined in figure 1 are shown in figure 3 to avoid ambiguities. The working distances for the two cameras are unequal, which accounts for the difference in the sizes of the two images. A time code generator (For-A VTG-33) displays elapsed time on the

monitor. The composite image is recorded by a SVHS video recorded (Sharp XC-2500S).

Data analysis takes place during playback of the video recording. The flow data are digitized using a frame grabbing board (RasterOps Video Color Board 364) and an Apple Macintosh IIci computer. The stored images are then converted from 24 bits colour to 8 bits grey scale using Adobe Photoshop software (Adobe Systems Incorporated). A threshold grey level is set in software (Image, NASA), and the stored image is converted to a binary image that eliminates all of the field except the capsule. Then, the lengths of the major and minor axes and the orientation angle are determined from the binary image. Owing to the error in measuring the lengths of the major and minor axes of the capsule, the uncertainty in D_{12} is ± 0.01. The error in the orientation angle depends on the magnitude of the deformation of the capsule. For highly deformed capsules, the orientation of the major axis can be specified to within 1°. However, for slightly deformed capsules with $D_{12} < 0.05$, it is difficult to locate the major axis from the recorded image, and data for θ are not reported in these cases.

The capsules are made by conducting an interfacial polymerization reaction at the surface of a liquid drop. The chemistry of the reaction and the design of a special reactor to fabricate the capsules are described in the accompanying paper (Chang & Olbricht 1993). At rest, i.e. in the absence of flow, the capsules are very close to spheres and most have diameters that range between 2 and 3 mm. The viscosity of the fluid inside the capsules varies between 0.50 and 8.0 P, which is much smaller than the viscosity of the outer-phase liquid. The values of the viscosity ratio λ range from 0.004 to 0.08.

To start an experiment, a single capsule is immersed in the suspending fluid between the cylinders at a depth greater than one gap width. The capsule is moved by hand until it is in the field of view of the two video cameras. A computer program that controls the stepping motors is then started, and data acquisition begins. The rotation speeds of the cylinders are occasionally adjusted manually by small amounts to keep the capsule stationary within the field of view. In most of the experiments the motion and shape of the capsule is recorded during start-up of simple shear flow for various values of the shear rate. Recording continues until the capsule exhibits no further changes in shape. The flow is stopped, and then the process is repeated with the shear rate set to the next larger value. In most experiments, this was continued until the capsule failed and burst. In some instances, the flow was stopped and the capsule was allowed to relax to a rest shape before the flow was started at the next higher shear rate.

In principle, the results of small-deformation theory can be used to deduce the apparent elastic modulus of the membrane from measurements of the capsule shape as a function of shear rate. One of the goals of the experiment is to compare the resulting values with another value of the elastic modulus obtained from an independent measurement. Techniques to measure the elastic modulus of a capsule membrane have not been studied and documented as extensively as methods of measuring the interfacial tension of a liquid drop for the corresponding drop deformation problem. Chang & Olbricht (1993) used a method based on squeezing the capsule between two parallel plates under a known load. An analysis of the problem by Feng & Yang (1973) and by Lardner & Pujara (1977, 1978, 1980) allows the elastic modulus Eh to be determined from the measured capsule shape and the known applied force. The measurement must be carried out for the same capsule used in the flow experiment, because the capsules formed in a single batch by the interfacial polymerization described in Chang & Olbricht differ from each other in membrane properties.

The usual protocol consisted of measuring the value of Eh in the squeezing

experiment and then conducting a Couette flow experiment using the same capsule. The squeezing experiment is described in detail in Chang & Olbricht (1993). Briefly, the capsule is placed in a Lucite box filled with polybutene, and a modified DuNuoy tensiometer is used to squeeze the capsule between parallel plates and, simultaneously, to measure the applied force. Because the polybutene is very viscous, adequate time must be allowed for the capsule shape to come to equilibrium. The shape is recorded on videotape and analysed later to determine Eh.

3. Results

In this section we present results that are representative of observations made for many capsules. More comprehensive results are presented in Chang (1991).

Figure 4 contains photographs of a capsule with $\lambda = 0.0038$ for five values of the shear rate G in the range $0 < G < 3.5\ \mathrm{s}^{-1}$. Figure 4(*a*) shows the capsule at rest just before the experiment starts. The capsule is very slightly deformed at rest, corresponding to a value of D_{12} of 0.02, which is an unavoidable consequence of handling the capsule in the viscous suspending fluid. Figure 4(*b*) shows the capsule in simple shear flow for $G = 0.25\ \mathrm{s}^{-1}$. Its projected shape closely resembles an ellipse, which is the shape predicted from the small-deformation theory. The measured value of D_{12} is 0.06, and the orientation angle θ is about 45°. The orientation angle θ is defined with respect to the streamlines of the undisturbed flow, which are in the vertical direction in the photographs (cf. figure 3). Figures 4(*c*) and 4(*d*) show the capsule for $G = 0.53$ and $0.97\ \mathrm{s}^{-1}$, respectively. It retains its elliptical shape, and the deformation increases with increasing shear rate. The measured values of D_{12} for these two cases are 0.13 and 0.17, respectively. Figure 4(*e*) shows the capsule for the largest shear rate, $G = 3.5\ \mathrm{s}^{-1}$. The shape deviates slightly from an ellipse in this case, which is evident from a lack of fore–aft symmetry along its major axis. The reason for an asymmetric shape is unknown, but it may be a consequence of the variation in shear rate across the capsule, which increases with capsule deformation, as given in (1). Ignoring this deviation and measuring approximate major and minor axes yields a value of 0.42 for D_{12}.

Although it cannot be seen from the photographs in figure 4, a close examination of the video recording reveals that capsule shape is not perfectly stationary in time. To illustrate the unsteadiness in the capsule shape, the capsule shown in figure 4(*e*) was photographed again 1.3 s later, and the result is shown in figure 4(*f*). Even though the shear rate was held fixed at $G = 3.5\ \mathrm{s}^{-1}$, the length of the major axis of the capsule decreased and the length of the minor axis increased during the interval between the two photographs. This is reflected in the value of D_{12}, which is 0.36 in figure 4(*f*) compared with 0.42 in figure 4(*e*). This difference is larger than the uncertainty in D_{12}, which is ± 0.01.

To show explicitly the time-dependent capsule deformation, the shape of the capsule shown in figure 4 was recorded continuously following the inception of simple shear flow for $G = 3.5\ \mathrm{s}^{-1}$. The results are shown in figure 5 in terms of D_{12} as a function of elapsed time from start-up at $t = 0$. The deformation of the capsule increases rapidly for short times, attaining a maximum at 0.4 s. Subsequently, the capsule shape oscillates about a mean deformation; the average value of D_{12} is 0.38, and the oscillatory part has an amplitude of 0.08 and a period of 2.1 s. Similar results are found for the same capsule for start-up with a slightly smaller shear rate of $3.2\ \mathrm{s}^{-1}$. For this case, the average value of D_{12} is 0.36, and the oscillatory part has an amplitude of 0.08 and a period of 2.5 s.

(a)

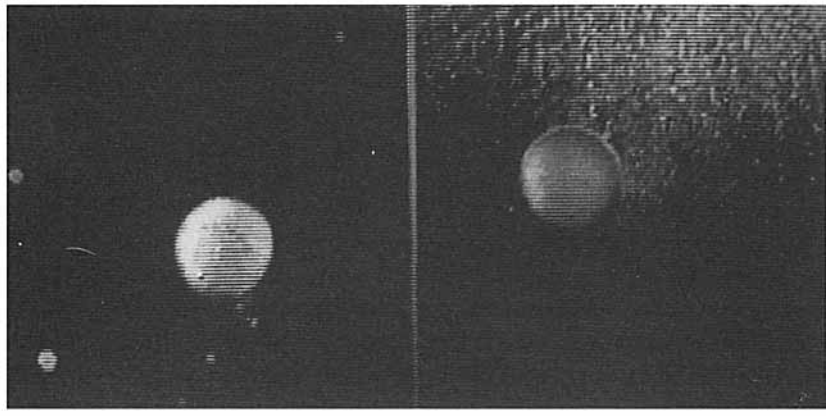

(b)

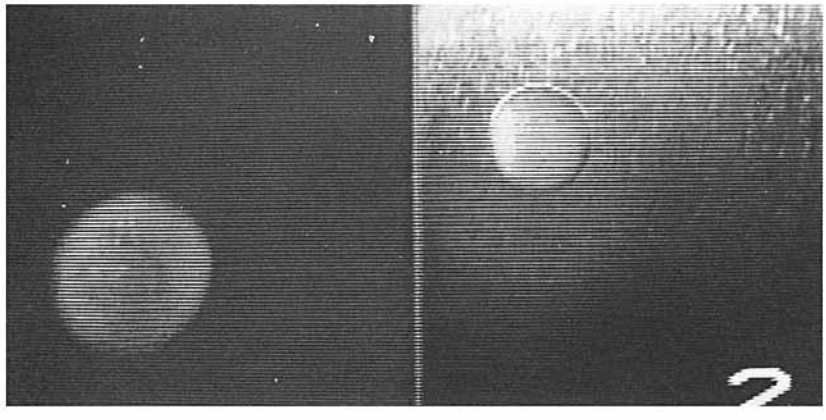

(c)

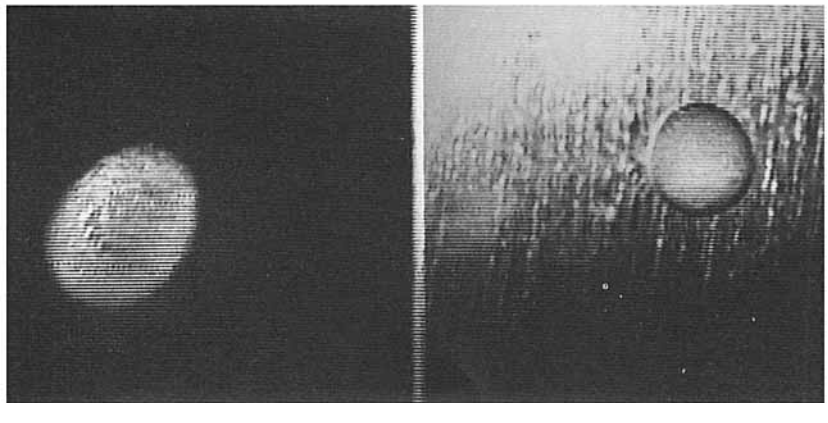

FIGURE 4(a–c). For caption see facing page.

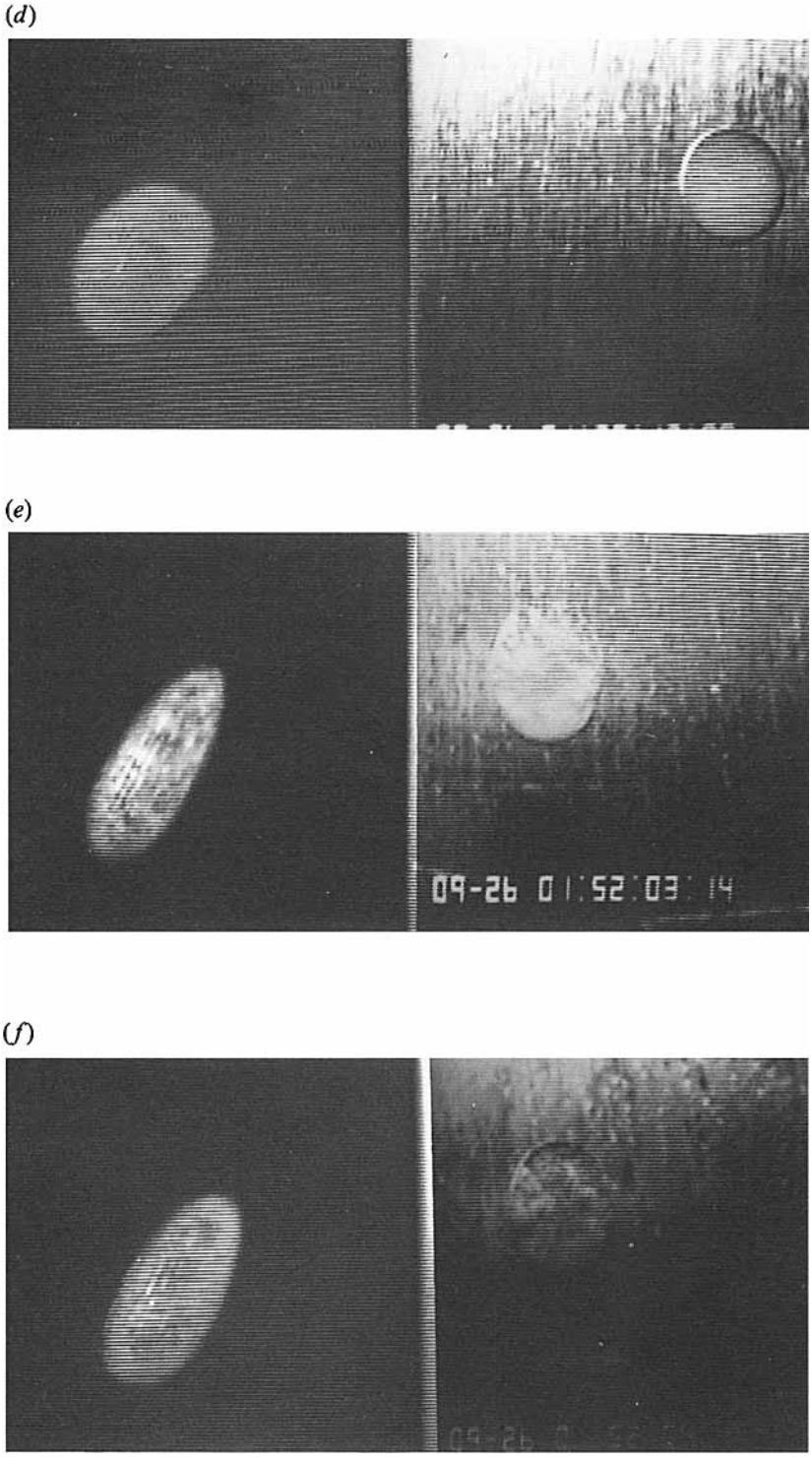

FIGURE 4. Top and side view photographs of a capsule with $\lambda = 0.0038$ for a series of shear rates. (*a*) Shows the capsule at rest before the experiment starts, $D_{12} = 0.02$; (*b*) $G = 0.25\ \text{s}^{-1}$, $D_{12} = 0.06$; (*c*) $G = 0.53\ \text{s}^{-1}$, $D_{12} = 0.13$; (*d*) $G = 0.97\ \text{s}^{-1}$, $D_{12} = 0.17$; (*e*) $G = 3.5\ \text{s}^{-1}$, $D_{12} = 0.42$; (*f*) the same capsule 1.3 s after the photograph in (*e*) was taken, $D_{12} = 0.36$.

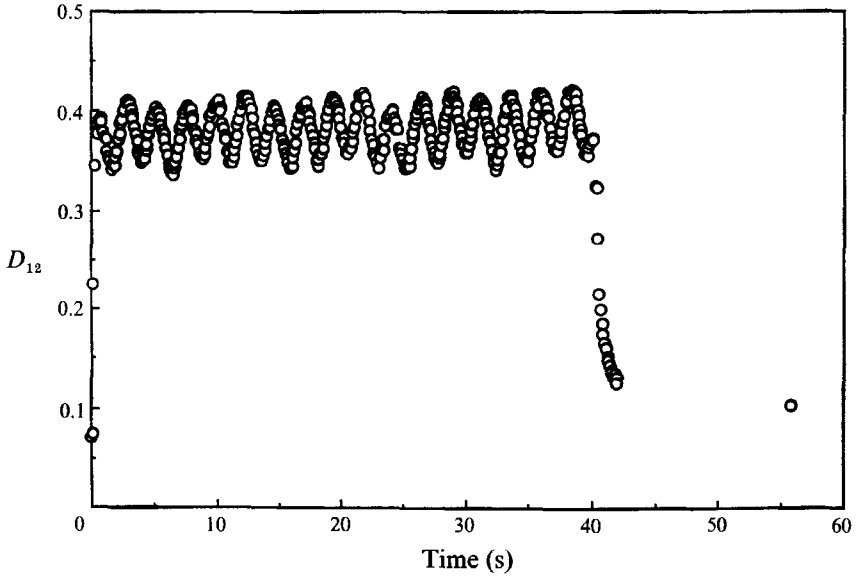

FIGURE 5. D_{12} as a function of elapsed time from start-up at $t = 0$ with $G = 3.5\ s^{-1}$.

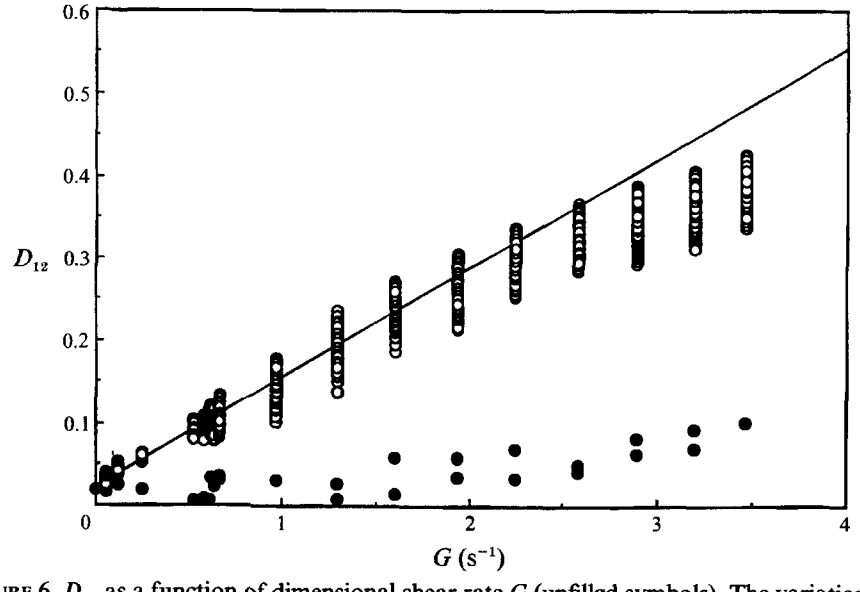

FIGURE 6. D_{12} as a function of dimensional shear rate G (unfilled symbols). The variation among the measured D_{12} values reflects discrete sampling of the time-dependent shape. The filled symbols give the value of D_{12} long after the flow is stopped as a function of the shear rate before the flow is stopped.

The relaxation of the capsule shape is shown in figure 5 after the flow is stopped at $t = 40.0$ s. It relaxes rapidly at first, and D_{12} decreases to 0.11 in 2.1 s. Further changes in the capsule shape take place much more slowly, and after 16 s, the deformation parameter reaches its final value of 0.09. A similar result is obtained for the smaller shear rate, although the residual deformation is 0.07 in that case. The fact that the capsule shape does not return to its original rest shape suggests that it may undergo a plastic deformation, which was also observed for capsules in hyperbolic extensional flow (Chang & Olbricht 1993).

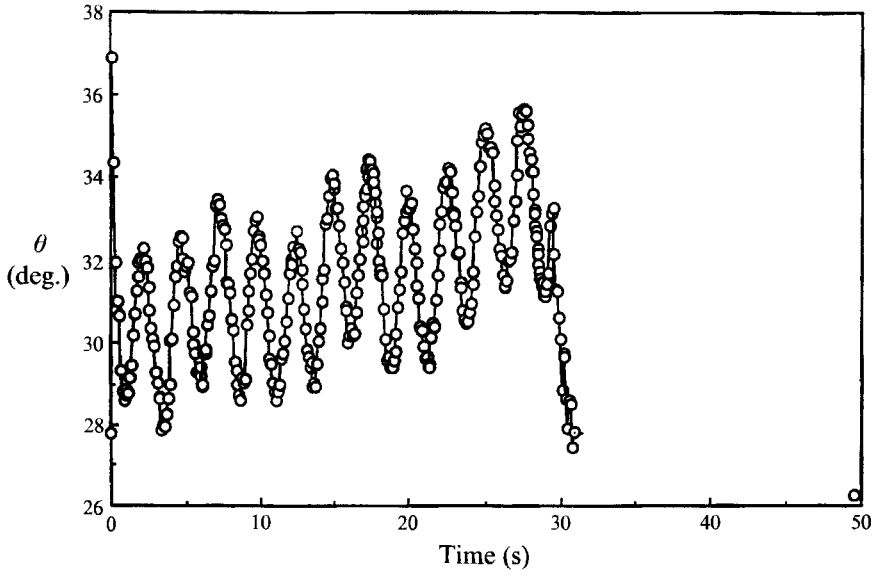

FIGURE 7. The orientation of the capsule as a function of time measured by the angle θ between the major axis of the capsule and the streamlines of the undisturbed flow for $G = 3.5\ s^{-1}$.

Figure 6 summarizes these results in terms of the deformation D_{12} as a function of dimensional shear rate G. The variation among the measured values of D_{12} for a fixed shear rate reflects discrete sampling of the time-dependent shape. Between 50 and 150 values of D_{12} were read from the video-recording for each shear rate to guarantee that the complete range of D_{12} for each shear rate is reported in the figure. For low shear rates, the mean value of the deformation parameter increases linearly with G, and the magnitude of the time-dependent part of the deformation increases with G. However, for $G > 2\ s^{-1}$ there is a deviation from linear behaviour, and the magnitude of the time-dependent part is independent of G.

The permanent deformation of the capsule after the flow is stopped also is shown in figure 6. The value of D_{12} long after the flow is stopped is shown as a function of the shear rate just before the flow is stopped. For $G < 1.6\ s^{-1}$ the capsule shape returns to its original rest shape, but for larger values of G, a permanent deformation is observed that increases with G up to 0.09 for $G = 3.5\ s^{-1}$.

The orientation of the capsule, measured by the angle θ between its major axis and the streamlines of the undisturbed flow, varies slightly with time as shown in figure 7 for $G = 3.5\ s^{-1}$. The capsule orientation is a periodic function with the same period shown for D_{12} in figure 5. The orientation angle θ is shown as a function of shear rate in figure 8.

The results for this capsule are qualitatively similar to those obtained for many others, as described in detail in Chang (1991). However, the quantitative results, such as the values of the mean and oscillatory parts of D_{12}, differ among the capsules that are fabricated in the polymerization reactor described by Chang & Olbricht (1993). These quantitative differences probably reflect differences in the local conditions in the reactor when the capsules are formed, which, in turn, affect the material properties of their membranes. We now examine whether the small-deformation theory described developed by Barthes-Biesel and co-workers can be used to correlate data for different capsules and to analyse the influence of membrane properties on the response of capsules to an imposed flow.

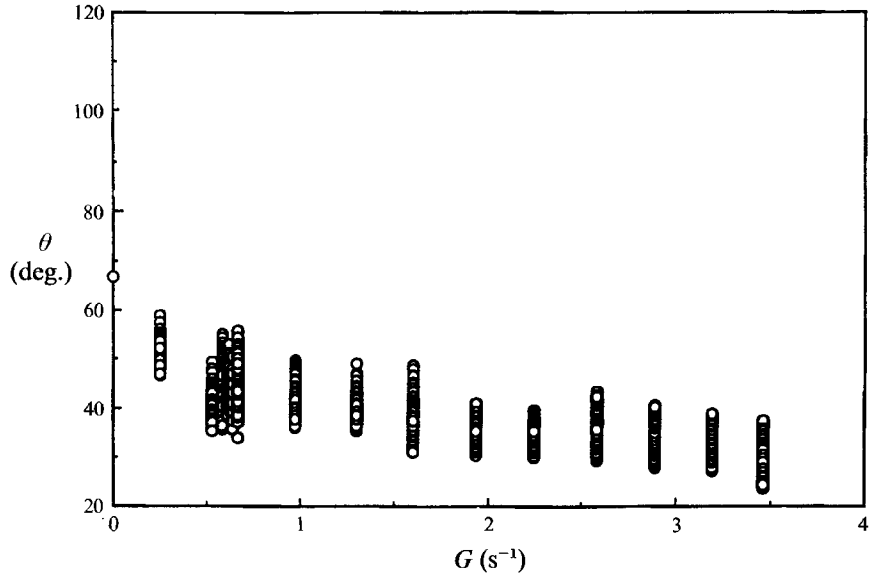

FIGURE 8. Orientation angle θ as a function of dimensional shear rate G.

4. Comparison of data with theory

4.1. *Results from small-deformation theory of Barthes-Biesel et al.*

The small-deformation theory for capsules follows closely the theory for the deformation of liquid drops. The liquid inside the capsule and the suspending liquid are assumed to be Newtonian, and the capsule Reynolds number, defined as $\rho Ga^2/\mu$ where ρ, the outer fluid density, is small. On the capsule surface, the velocity of the membrane matches the fluid velocity. The jump in the stress vector across the membrane is balanced by the force exerted by the membrane on the fluids. The stress field within the membrane depends on its constitutive behaviour.

Although several constitutive models for the capsule membrane have been analysed, including some with nonlinear properties, we examine results obtained by Barthes-Biesel & Sgaier (1985) for a linear viscoelastic membrane. The elastic response of the membrane is described by a strain energy function with coefficients that must be determined from experiments. For a three-dimensional, isotropic, incompressible membrane, which seems appropriate for the model capsules used in this experiment, these coefficients involve a single parameter E, the membrane Young's modulus. The membrane viscous response is characterized by two moduli: a shear viscosity and a dilatational viscosity. Since there is no information available concerning the relative magnitudes of the two moduli, they are set equal as a first approximation, and the membrane viscosity is characterized by a single coefficient, μ^s. The stress in the membrane is taken to be the Voigt sum of viscous and elastic contributions. Tensions in the membrane due to viscous effects are characterized by $\mu^s G$ and those due to elastic effects by Eh, the product of the Young's modulus and the membrane thickness.

Dimensional analysis shows that the capsule shape in simple shear flow depends on three dimensionless parameters: λ, the ratio of inner fluid viscosity to outer fluid viscosity; $\mu Ga/Eh$, the ratio of viscous forces exerted by the outer fluid on the membrane to elastic forces in the membrane; and $\mu^s/\mu a$, the ratio of membrane viscous modulus to viscous effects in the outer fluid. The parameter λ also appears in the problem of drop deformation and breakup, and $\mu Ga/Eh$ serves the same purpose here

as the capillary number does in the drop deformation problem, with Eh replacing the interfacial tension γ.

Barthes-Biesel & Sgaier (1985) solve the Stokes equations and boundary conditions for a capsule in a general linear flow by a regular perturbation expansion in the asymptotic limit of small deformations from a spherical rest shape. For viscosity ratios λ that are $O(1)$ or less, which is the case for all experiments in this study, the shape of the capsule does not depend on the exact value of λ. Still, there are three distinct small-deformation asymptotic limits. In every case, the calculated shape of the slightly deformed capsule in simple shear flow is an ellipsoid with principal diameters L and B in the shear plane.

The case $\mu Ga/Eh \ll 1$ and $\mu^s/\mu a = O(1)$ corresponds to weak flows or strong elastic forces in the membrane. The steady-state shape of the capsule to first order in $(\mu Ga/Eh)$ is an ellipsoid with its major axis oriented at an angle θ of 45° with respect to the undisturbed fluid streamlines. The deformation of the capsule D_{12} is

$$D_{12} = \tfrac{25}{4}(\mu Ga/Eh) + O(\mu Ga/Eh)^2. \tag{2}$$

Thus, for sufficiently small shear rates, the deformation D_{12} is predicted to be a linear function of $\mu Ga/Eh$, which immediately allows the elastic modulus Eh to be determined.

The case $\mu Ga/Eh \ll 1$ and $\mu^s/\mu a \gg O(1)$ corresponds to a viscous membrane with a large elastic modulus. The deformation of the capsule is

$$D_{12} = \frac{5(\mu Ga/Eh)[\beta^2(\beta^2+\frac{7}{9})^2 + (\beta^2+\frac{5}{9})^2/4]^{\frac{1}{2}}}{2(\beta^2+1)(\beta^2+\frac{1}{9})} \tag{3}$$

and the orientation angle θ is

$$\theta = \tfrac{1}{2}\arctan\frac{\beta^2+\frac{5}{9}}{2\beta(\beta^2+\frac{7}{9})}, \tag{4}$$

where β is the group $\mu^s G/Eh$. For large values of β, which can be obtained by increasing the shear rate, the deformation parameter D_{12} tends to a limiting value of $5\mu a/2\mu^s$. This result is qualitatively different from the case of a purely elastic membrane, where no limit in deformation is found as the shear rate is made large. In principle, the viscous modulus of a viscoelastic membrane can be deduced from the large-shear-rate asymptote of D_{12}.

The third case is given by $\mu Ga/Eh = O(1)$ and $\mu^s/\mu a \gg O(1)$, which corresponds to a highly viscous membrane. In this case, the capsule exhibits a periodic shape in steady simple shear flow. The deformation parameter and orientation angle are given as the following functions of time t:

$$D_{12} = m(\mu a/\mu^s)\sin(\tfrac{1}{2}t) \tag{5}$$

and

$$\left.\begin{aligned} \theta &= \tfrac{1}{4}\pi - \tfrac{1}{4}t, \quad t \in [0, 2\pi] \bmod 4\pi, \\ \theta &= \tfrac{3}{4}\pi - \tfrac{1}{4}t, \quad t \in [2\pi, 4\pi] \bmod 4\pi, \end{aligned}\right\} \tag{6}$$

where m is a constant that depends on the particular strain energy function for the material.

4.2. *Comparison with theory – low shear rates*

An examination of figure 6 shows that if the variation in D_{12} for a fixed value of G is temporarily ignored, then the data resemble qualitatively the predicted behaviour for a capsule with a viscoelastic membrane. For small values of G, D_{12} increases linearly

Capsule	Eh (dyn/cm) deformation	Eh (dyn/cm) simple shear	μ_i (P)	μ_o (P)	$2a$ (cm)
1	710	1130	0.50	132	0.36
2	620	840	0.50	127	0.38
3	1370	1570	0.50	125	0.38
4	1030	1100	0.66	129	0.38
5	330	580	0.65	96	0.49
6	520	540	0.66	112	0.46
7	380	560	0.65	96	0.46
8	260	550	0.65	93	0.46
9	260	750	0.65	84	0.46
10	740	930	8.0	112	0.47
11	380	980	8.0	112	0.48
12	940	1270	8.0	107	0.44
13	1160	1220	8.0	112	0.43
14	620	1130	8.0	112	0.37
15	430	930	8.0	107	0.46
16	480	850	8.0	107	0.38

TABLE 1. Values of the membrane elastic modulus determined from the capsule squeezing experiment compared with those determined from the deformation in simple shear flow. μ_i and μ_o are the viscosities of the inner- and outer-phase fluids

with G as shown by the line drawn through the median value of D_{12} for each shear rate. Identifying this line with the small-deformation result given by (2) yields a value of 1130 dyn/cm for the elastic modulus Eh of the capsule. With this modulus, the resulting value of $\mu Ga/Eh$ ranges from zero to 0.04 over the linear portion of the data ($G < 2\ s^{-1}$), which satisfies the weak-flow-limit constraint $\mu Ga/Eh \ll 1$.

Although this shows the procedure to determine Eh is self-consistent, a more stringent comparison between experiment and theory is to compare the resulting value of Eh with the value obtained in the squeezing experiment for the same capsules. For the capsule in the present experiment, the resulting value from the squeezing experiment is 710 dyn/cm.

Results for other capsules follow the same qualitative trend. Table 1 presents a summary for capsules with measured values of Eh that range from 260 to 1570 dyn/cm. In every case, a fit of data for D_{12} to the result given in (2) yields a value of Eh that is larger than the value measured for the same capsule in the squeezing experiment. The discrepancy is too large to be attributed to higher-order terms in the small-deformation expansion. The differences between the values of Eh measured by the two different techniques are not necessarily surprising, because they are comparable in magnitude to differences among measurements of the elastic modulus of solid polymers using different techniques (Rodriguez 1982). However, at least part of the difference between the measured values appears to be systematic, insofar as the flow experiment yields a larger Eh than the deformation experiment in every case.

The difference in values from the two techniques may involve the chemical properties of the membrane and certain characteristics of the measurements. The capsule membrane is a derivative of nylon formed from diethylene triamine, a monomer with three functional groups. More common nylons, including commercial nylons such as nylon 6-10, are formed from monomers with two functional groups, e.g. hexamethylene diamine, which assures end-to-end polymerization. The presence of the third amine

Case	D_{12c}	μ^s (P cm)	μ^s_{fit} (P cm)
1	0.45	130	—
2	0.36	160	—
3	0.42	140	120
4	0.42	150	130
5	0.44	130	120
6	0.56	120	100
7	0.46	120	90
8	0.44	120	90
9	0.53	90	70
10	0.55	120	100
11	0.48	140	120
12	0.48	120	120
13	0.52	110	100
14	0.50	100	90
15	0.44	140	110
16	0.50	100	90

TABLE 2. Values of membrane viscosity μ^s determined from fitting experimental data to small-deformation theory.

group probably promotes extensive cross-linking of the nylon chains that results in the formation of an amorphous polymer. Measurements of the elastic modulus of amorphous polymers often exhibit time-dependent results, especially for materials near their glass transition temperature. Owing to the fact that the material has a wide distribution of relaxation times, the *apparent* Young's modulus decreases as the characteristic time of the experiment increases (e.g. Rodriguez 1982). The magnitude of the effect depends strongly on temperature and is largest in the glass transition region.

The two techniques used to measure Eh in this experiment have very different timescales. The characteristic time of membrane stretching and relaxation in simple shear flow is the membrane rotation time, which varies with shear rate between $O(1)$ and $O(10)$ s for the conditions in this experiment. However, the experiment involving the deformation of the capsule between parallel plates takes place much more slowly, owing to the large viscosity of the outer phase liquid, with a characteristic time on the order of 10^2 s. For a material near its glass transition, we expect the simple shear flow experiment to yield a larger value for the apparent elastic modulus than the deformation experiment, which is the qualitative result we find.

4.3. *Comparison with theory – high shear rates*

The theory for a capsule with a viscoelastic membrane predicts that deformation at high shear rates is limited by membrane viscosity. For the case $\mu Ga/Eh \ll 1$ and $\mu^s/\mu a \gg O(1)$, the high-shear-rate asymptote for D_{12} is $5\mu a/2\mu^s$. Applying this result to the deformation D_{12} for the largest shear rate in figure 6 gives a value of μ^s of 130 P cm. If μ^s is determined by fitting data for D_{12} to theory over the entire range of shear rates covered in the experiment, the resulting value of μ^s does not change significantly. The values for μ^s for a collection of capsules are listed in table 2. In some cases, the limiting deformation was not attained in the experiment. In these cases the values of μ^s obtained from a fit over all shear rates differ by up to 20% from the values obtained by applying the asymptotic relation. In applying the small-deformation theory, we note

that the constraint on the dimensionless shear rate, $\mu Ga/Eh \ll 1$, is satisfied because $\mu Ga/Eh$ is less than 0.1, even for the largest shear rate. However, D_{12} reaches values of up to 0.4, which suggest that the deformation is not small, even at relatively low dimensionless shear rates. Nevertheless studies of deformable liquid drops and the accompanying study of capsules in extensional flow show that the small-deformation theory can be accurate for surprisingly large deformations of the drop or capsule.

These results for the membrane viscosity are deduced from the values of D_{12} in steady simple shear flow (ignoring the small oscillation in shape). However, it remains to be determined whether the resulting values are quantitatively consistent with other aspects of the capsule response, such as the shape in an unsteady flow following start-up of simple shear. According to the small-deformation theory, the membrane viscosity influences the capsule shape for short times after the start-up of simple shear flow, even under circumstances when the membrane viscosity does not affect the steady-state shape of the capsule, e.g. in the weak-flow limit. The shape for short times is determined by two time constants, μ^s/Eh and $3\mu^s/Eh$, which correspond to two modes of deformation, pure shear and area dilatation, respectively. Taking $\mu^s =$ 120 P cm and $Eh = 600$ dyn/cm as representative values gives time constants of 0.2 and 0.6 s. These timescales are consistent with the rise times for D_{12} in figure 5 following start-up of simple shear, which lends support to the measured values of μ^s. Indeed, under no circumstance for any capsule or for any shear rate that was tested were the results deduced from steady-state shapes inconsistent with the time-dependent response.

Finally, the small-deformation theory for a viscoelastic membrane gives θ in terms of the dimensionless parameter $\beta = \mu^s G/Eh$ according to (4). The orientation angle θ decreases from 45° at $\beta = 0$ to 0° at infinite β according to the theory. The data follow the same qualitative trend, although measurements of the orientation are subject to relatively large uncertainties for small shear rates. The minimum value of β attained for the data shown in figure 8 at the highest shear rate in the experiment is 0.40. The small-deformation theory predicts that θ is 22°, but the measured values of θ range between 22° and 38° as the capsule shape changes periodically.

The periodic variation of the capsule shape is perhaps the most significant discrepancy between the small-deformation theory for a viscoelastic capsule and the experimental data. The theory predicts that the shape should have a damped oscillation following the start-up of simple shear flow, but it should decay over a time of $O(\beta)$, which is small compared with the observation time in the experiment. Instead, the data for D_{12} show an oscillation that does not decrease with time.

The asymptotic limits that lead to small deformations depend on $\mu Ga/Eh$ and $\mu^s/\mu a$. If $\mu Ga/Eh$ is sufficiently small, the deformation of the capsule is limited by the elastic modulus of the membrane. In this limit, the capsule exhibits a steady shape, regardless of the value of $\mu^s/\mu a$. However, if $\mu Ga/Eh$ is made sufficiently large, $O(1)$ according to theory, then the capsule deformation is small only if $\mu^s/\mu a \gg O(1)$. In this case, the deformation is limited by the membrane viscosity, and the capsule shape is periodic. To estimate $\mu^s/\mu a$ in this experiment, we note that the membrane viscosity μ^s is about 120 P cm and does not vary much among the capsules, the outer liquid viscosity is about 100 P, and the capsule radius is about 0.2 cm. Thus, a typical value of $\mu^s/\mu a$ is about 6 and is independent of the shear rate. On the other hand, $\mu Ga/Eh$ varies with shear rate from zero to a maximum of about 0.2 in this experiment. Even though 0.2 does not seem large at first glance, $\mu Ga/Eh$ is analogous to a capillary number in the drop deformation problem, and 0.2 is a relatively large value in that case. Thus, it is possible that the deformation of the capsule is limited, at least in part, by the

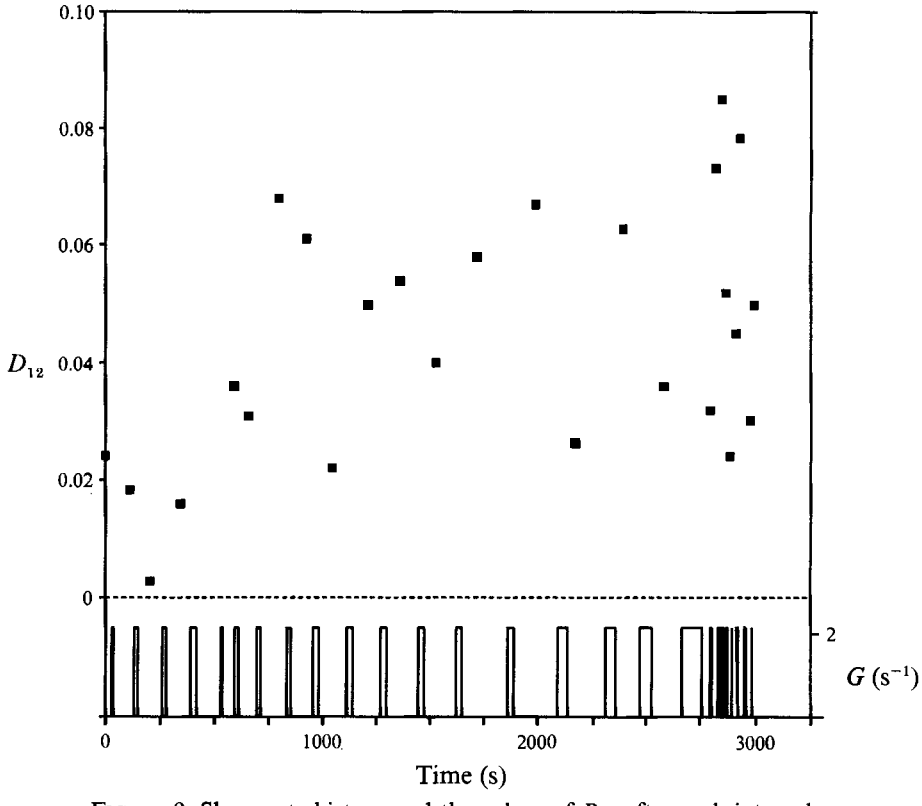

FIGURE 9. Shear rate history and the values of D_{12} after each interval.

membrane viscosity. In the limit of a purely viscous membrane, the small-deformation theory predicts an unsteady capsule shape with period $2\pi/G$ to within a small correction, which agrees with experimental observations. However, the predicted magnitude of the oscillatory part is much larger than that observed in the experiments, since the capsule is supposed to pass through a spherical shape in each oscillation, according to theory for a purely viscous membrane.

It is possible that the results resemble a case intermediate between elastically limited deformation and membrane viscosity-limited deformation, but the small-deformation theory still predicts a steady capsule shape to the order at which the calculations have been carried out. It is possible that the observed unsteadiness in the shape is a consequence of higher-order terms neglected in the theory. The largest of these is $O(\mu^s/\mu a)^{-1}$, about $\frac{1}{6}$. It seems possible that unknown terms of this magnitude could modulate the lengths of the capsule major and minor axes by about 10%, which is enough to account for the observed oscillation in D_{12}, but further analysis of the small-deformation limit is required to prove this.

4.4. *Flow-induced permanent distortion of the capsule*

The suspended capsules exhibit a permanent distortion in rest shape that is similar to the distortion shown by capsules in hyperbolic extensional flow (Chang & Olbricht 1993). The magnitude of the distortion is shown in figure 6. For small shear rates, the rest shape is a sphere to within the experimental error in D_{12} of ± 0.01. However, for sufficiently large shear rates, say $\mu Ga/Eh \geqslant 0.04$, the rest shapes show significant deviations from sphericity. The permanent deformation increases with the magnitude

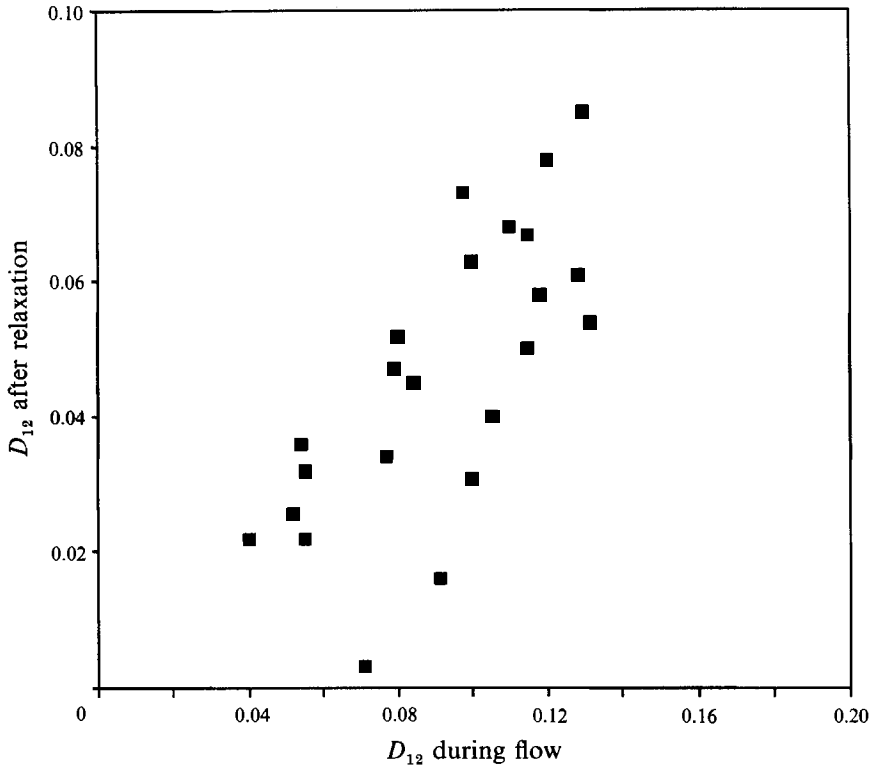

FIGURE 10. Correlation of the shape of the capsule at the instant the flow was stopped with its shape long after the capsule has fully relaxed.

of the shear rate just before the flow was stopped. In most of our experiments, the shear rate was increased in increments, and the exposure time of the capsule to the flow was not necessarily identical for all the shear rate values.

Therefore, we investigated the permanent distortion of some capsules under controlled conditions and for larger shear rates. A capsule was exposed to intervals of flow with the shear rate G set to a relatively large value of 2 s^{-1}. After each interval the capsule shape was allowed to relax completely and the permanent distortion was measured. The results are presented in figure 9, where the shear rate history and the values of D_{12} for the capsule at rest after each interval are shown. The distortion from a spherical rest shape is not significant until after six intervals (700 s) of exposure. After that, the distortion at rest ranges between 0.02 and 0.09. The magnitude of D_{12} after each interval does not depend on the total strain exposure. Furthermore, the magnitude of the distortion at rest decreases in some instances as a result of additional exposure to the flow. Combining the results in figure 9 with those in figure 6, we conclude that the amount of permanent distortion of the capsule depends on shear rate, but not on total strain, provided the total strain is above some minimum, which is $2\ s^{-1} \times 62\ s = 124$ for the example shown in figure 9.

To explore further the variations in the measured values of D_{12} at rest, we correlated the rest shape of the capsule with its shape at the instant the flow was stopped. The results are shown in figure 10, which maps the data in terms of the value of D_{12} just before the flow was stopped and the final value of D_{12} measured long after the flow was stopped. The data suggest a reasonably strong correlation between the rest shape distortion and the flow-induced deformation, with a correlation coefficient of 0.58.

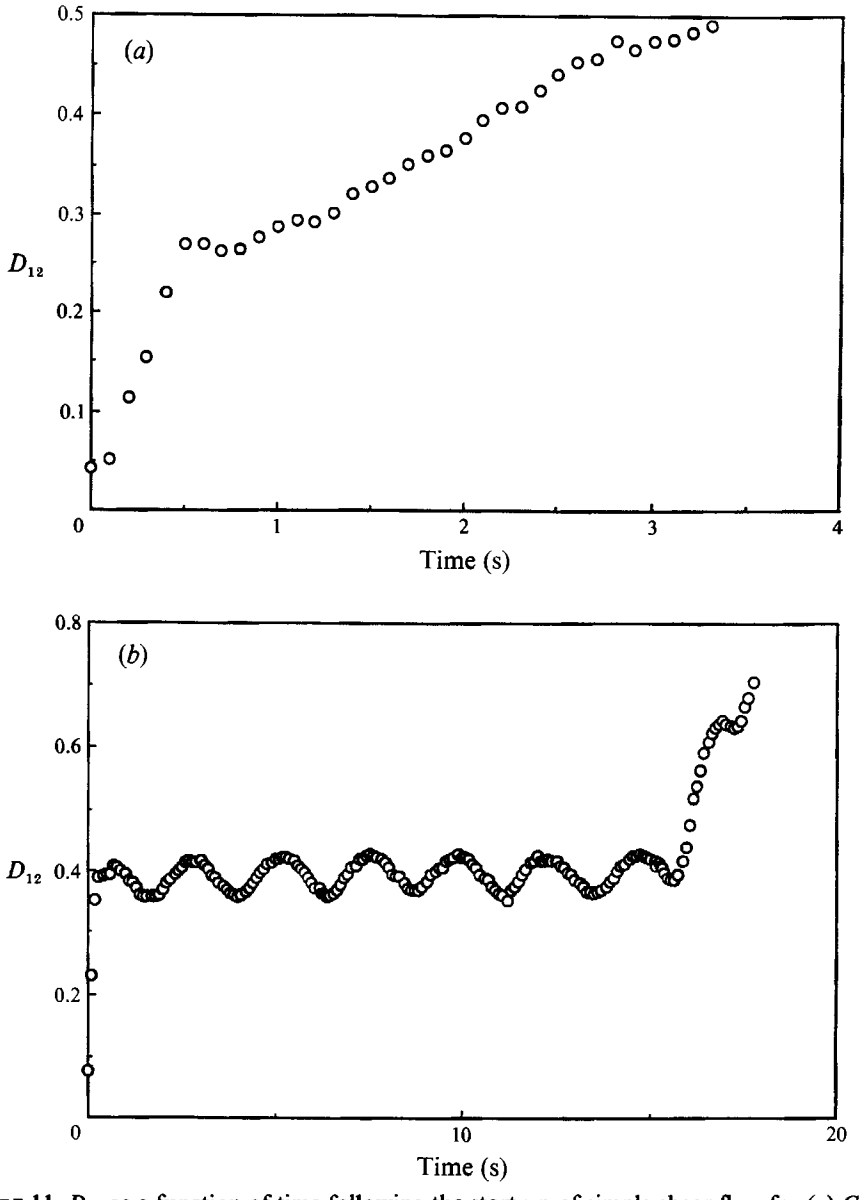

FIGURE 11. D_{12} as a function of time following the start-up of simple shear flow for (*a*) $G = 2.32\ s^{-1}$, which corresponds to a value of $\mu Ga/Eh$ of 0.066; (*b*) $G = 3.50\ s^{-1}$, which corresponds to a value of $\mu Ga/Eh$ of 0.10.

Furthermore, although it cannot be seen from the figure, the orientation of the major axis of the capsule at rest also is strongly correlated with the orientation of the major axis of the capsule in flow just before the flow is stopped (Chang 1991). These results suggest that if some flow-induced structural change within the membrane is responsible for the permanent distortion of the rest shape, as suggested by Chang & Olbricht (1993), it is at least partially reversible by exposing the capsule to the flow again. In fact, the spherical shape of the capsule at rest can be almost recovered by stopping the flow at opportune times when the value of D_{12} under flow is a minimum.

The dimensionless shear rate required for permanent deformation is much higher in

(a)

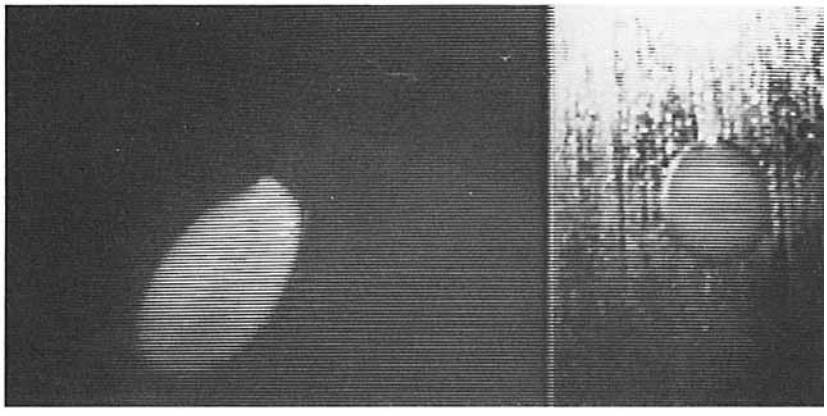

(b)

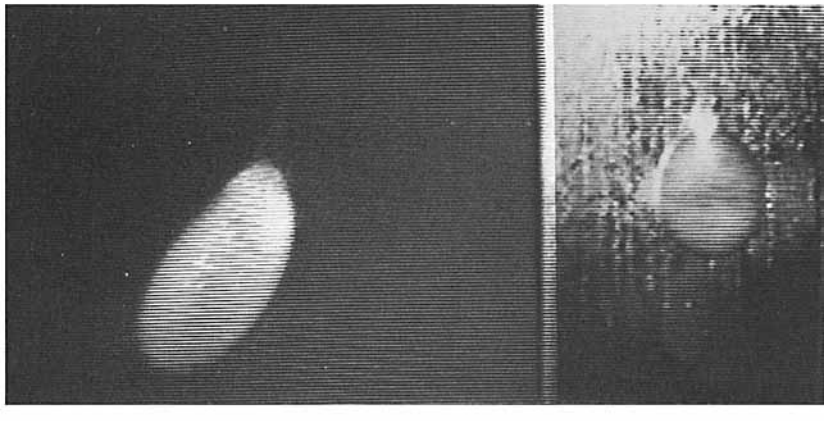

(c)

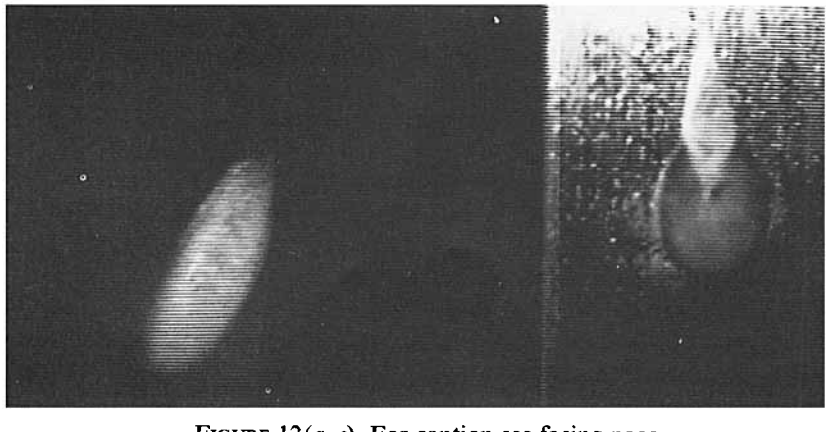

FIGURE 12(a–c). For caption see facing page.

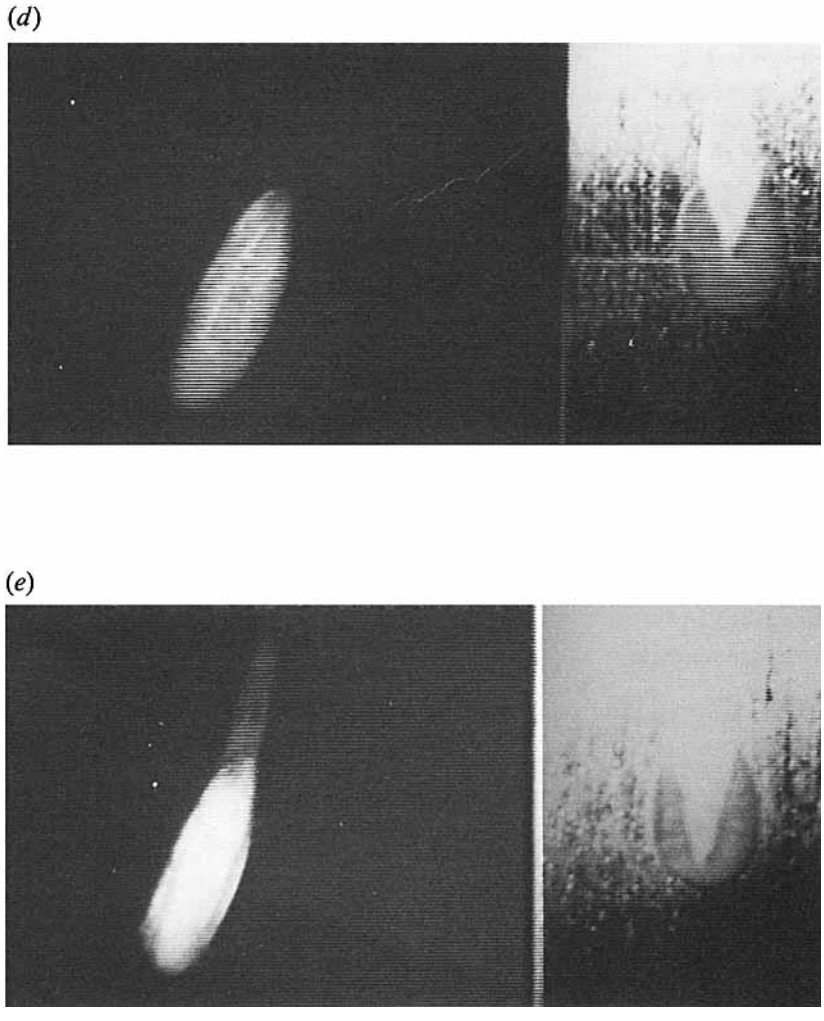

FIGURE 12. A sequence of video monitor images showing capsule breakup. (*a*) The capsule at the first indication of breakup defined as $t = 0$; (*b*) $t = 0.40$ s; (*c*) 1.50 s; (*d*) 2.00 s; (*e*) 3.00 s.

simple shear flow than in purely extensional flow. A typical value of the dimensionless shear rate $\mu Ga/Eh$ for the capsule to achieve a detectable permanent deformation in simple shear flow is about 0.03. For the case of pure straining flow, the minimum dimensionless shear rate required is 0.002. This difference is attributed to the irrotational kinematics of the extensional flow and the fact that the membrane does not rotate in purely extensional flow.

5. Capsule breakup

When the flow-induced deformation of the capsules in simple shear flow was made sufficiently large by increasing the shear rate, the capsule broke in every case that was studied.

Figure 11(*a*) shows D_{12} as a function of time following the start-up of simple shear flow with $G = 2.32\ \text{s}^{-1}$, which corresponds to $\mu Ga/Eh = 0.066$ for this particular capsule. The deformation parameter D_{12} increases to a local maximum at 0.5 s. The

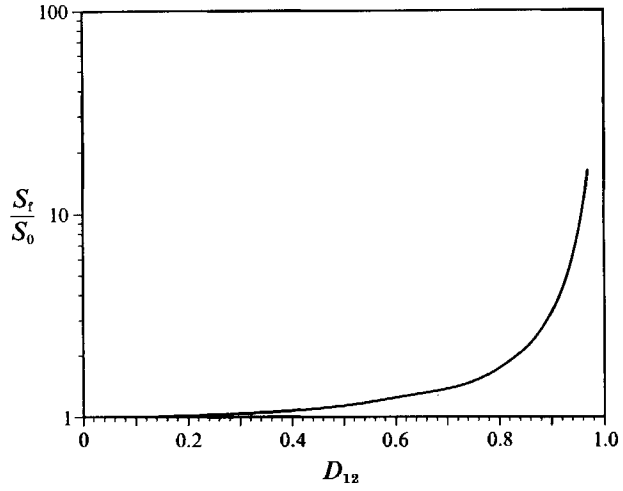

FIGURE 13. The ratio S_f/S_0, the surface area of the deformed capsule to the area of the undeformed capsule, as a function of the deformation parameter D_{12}.

time constant $3\mu^s/Eh$ in this case is 0.57 s. However, instead of oscillating about a mean value, the capsule stretches until the membrane bursts and the contents of the capsule spill into the suspending fluid. Figure 11(*b*), which pertains to another capsule, shows that breakup can occur after several oscillations in shape for sufficiently large shear rates.

Figure 12 shows a sequence of video monitor images during breakup of a capsule. Figure 12(*a*) shows the capsule at the first indication of breakup, which is set arbitrarily to $t = 0$. The left image is a top view of the capsule with deformation parameter $D_{12} = 0.26$. The right image is a side view showing breakup starting near the top of the capsule along the x-axis ($z = 0$). This corresponds to the tip of the major axis in the top view. Here, as in most cases, breakup occurs when a thin strip of the membrane in the (x, y)-plane near the tip of the major axis tears open. Figure 12(*b*) (right) shows that the tear propagates in the positive x-direction, which is the direction of membrane rotation. Figure 12(*b*) (left) shows that even as the tear grows, the overall membrane shape remains relatively unchanged. However, liquid inside the capsule is spilling through the tear into the outer liquid. Figure 12(*c–e*) (right) shows that the tear continues to grow until the capsule is split along the positive x-axis. Figure 12(*c–e*) (left) shows that the capsule continues to elongate as it tears. Eventually, the capsule splits into two pieces, one of which leaves the field of view in the positive x-direction, while the other leaves in the negative x-direction. In fact, the symmetry of the flow suggests that tearing is just as likely to start at the opposite end of the major axis. Indeed, tearing was equally likely to start at either end of the major axis among many capsules that were studied. The critical value of the deformation at breakup, say D_{12c}, is shown in table 2. The breakup of capsules in simple shear flow is considerably different from the breakup observed by Barthes-Biesel (1991) in extensional flow. Polylysine capsules in hyperbolic extension developed pointed ends along the principal strain axis that formed leaks in the capsule membrane.

Since capsule breakup starts at specific points on the membrane surface, it seems appropriate to examine the local deformation at these particular points. Unlike the capsule membrane used in theoretical studies of breakup (e.g. Li, Barthes-Biesel & Helmy 1988), which is an infinitely thin sheet of an elastic material, the experimental

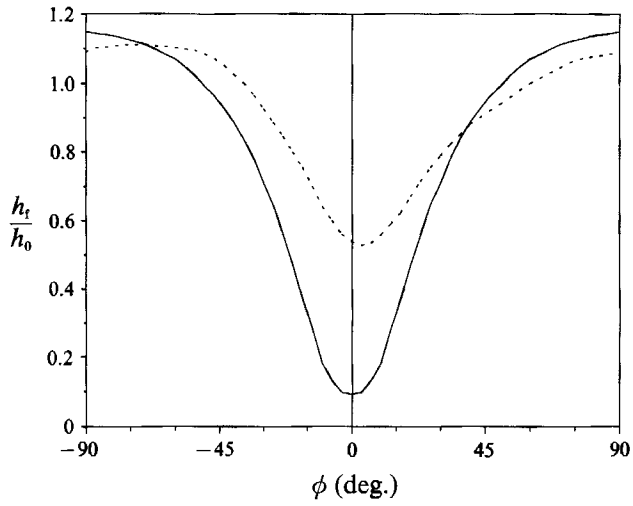

FIGURE 14. The ratio h_f/h_0, the membrane thickness of the deformed capsule to the membrane thickness of the undeformed capsule, as a function of position specified by ϕ, which is defined in figure 1, in degrees: --, $D_{12} = 0.4$; ——, $D_{12} = 0.6$.

capsule has a finite membrane thickness that may vary around the surface when the capsule is deformed. If the total surface area of the capsule increases as it deforms, conservation of membrane volume requires that the average membrane thickness decreases. The change in the average membrane thickness due to capsule deformation can be calculated from the geometry of the capsule. The ratio of the total surface area S_f of a deformed capsule to the surface area S_0 of a spherical capsule is shown in figure 13 as a function of the deformation parameter D_{12}. The total surface area of the capsule does not increase appreciably unless D_{12} exceeds 0.8, a value that is not attained in the experiments. For $D_{12} = 0.6$, S_f increases by about 20%, which implies a relatively small change in the average membrane thickness. Nevertheless, the capsules tend to break for values of D_{12} between 0.4 and 0.6.

Although the decrease in the average membrane thickness is less than 20%, local changes may be much larger. To estimate the local change in the surface area, and hence the local change in membrane thickness, we use the local membrane deformation calculated by Barthes-Biesel & Sgaier (1985):

$$A \equiv \log \lambda_1 \lambda_2 = \tfrac{1}{2}\log\{\tfrac{1}{2}[\mathrm{tr}(\boldsymbol{A}\cdot\boldsymbol{A}^{\mathrm{T}})]^2 - \tfrac{1}{2}\mathrm{tr}[(\boldsymbol{A}\cdot\boldsymbol{A}^{\mathrm{T}})^2]\}, \tag{7}$$

where the local surface area change is given by the invariant A_1. In (7), λ_1 and λ_2 are principal extension ratios and $\boldsymbol{A}$ is a two-dimensional deformation tensor. This equation can be rewritten as

$$A \equiv \log \lambda_1 \lambda_2 = \epsilon \boldsymbol{x}\cdot(2\boldsymbol{J} - 3\boldsymbol{K})\cdot \boldsymbol{x} + O(\epsilon^2), \tag{8}$$

where ϵ is the small parameter $[Eh/\mu Ga + \mu^s a/\mu]^{-1}$, $\boldsymbol{x}$ is a position vector originating at the centre of the capsule, and $\boldsymbol{J}$ and $\boldsymbol{K}$ are symmetric, traceless tensors calculated by Barthes-Biesel & Sgaier. Knowing a, μ, μ^s, Eh and G, we can calculate the local surface area change $\lambda_1\lambda_2$ as a function of position on the surface for a given value of G or D_{12}. Applying conservation of volume leads to the local value of the membrane thickness h_f.

The results of the calculation are shown in figure 14 for $D_{12} = 0.4$ and 0.6. The ratio h_f/h_0, the local thickness of the deformed capsule to the thickness of the undeformed

capsule, is shown for a strip of the membrane in the shear plane containing the centre of mass of the particle. The angle ϕ, which is defined in figure 1, is drawn counterclockwise with $\phi = 0$ corresponding to the principal major axis of the capsule. For both values of D_{12}, the minimum membrane thickness occurs very near the major axis of the capsule. This is very close to the location where breakup starts. The minimum thickness is a strong function of deformation; for $D_{12} = 0.4$ the minimum thickness is about $0.55h_0$, and for $D_{12} = 0.6$, it is $0.1h_0$. The usefulness of the results is mainly qualitative for such large deformations. In any event, the maximum thickness of the membrane occurs near the minor axis of the capsule, where the membrane locally is under compression.

It thus appears that membrane rupture is strongly correlated with thinning of the membrane at points where the local deformation is the largest. Unfortunately, no direct measurement of the membrane thickness at breakup is possible. However, Chang (1991) conducted additional tests of membrane deformation by drawing a small portion of the capsule membrane into a micropipette under suction. The results showed that as the piece of the membrane covering the pipette entrance is drawn into the pipette, its surface area changes. Assuming that the thickness remains constant over the piece, the change in thickness can be calculated. If the suction drawing the membrane into the pipette is made sufficiently large, the membrane will break. Results for several capsules show that breakup occurs when the membrane thickness decreases to about 0.50 of its original (undeformed) thickness.

6. Conclusions

These experiments describe an attempt to study systematically the motion, deformation, and breakup of encapsulated particles in well-defined flows. The model capsules used in the study are of sufficient size and stability that the dynamics of capsule motion can be visualized directly.

The flow-induced deformation of the capsules in simple shear flow follows the predictions of the small-deformation theory worked out by Barthes-Biesel & Sgaier for capsules with viscoelastic membranes. Using the theory to correlate data for the steady-state shape of the capsule leads to values of the elastic modulus of the membrane that are reasonably well correlated with measurements from an independent experiment, namely the deformation of the capsule between two parallel plates under a known load. Comparison of the data with theory also yields the value of the membrane viscosity. The major difference between the behaviour of the capsules in simple shear flow and the predictions of the theory is that the capsules exhibit a small oscillation in their shape about a mean deformation, whereas the theory predicts that the shape should be steady.

The experiments demonstrate that the capsule membrane exhibits nonlinear constitutive behaviour for sufficiently large rates of deformation. The membrane undergoes an anisotropic plastic deformation that causes the capsule to have a non-spherical shape and a preferred orientation after the flow is stopped. For the largest shear rates obtained in the experiments, the capsules burst by membrane failure that occurs at the point where the membrane undergoes its maximum extension. Breakup of the capsule is strongly correlated with thinning of the membrane owing to flow-induced deformation.

The experiments suggest that the small-deformation theory can be used to predict the rheological properties of viscoelastic synthetic capsule membranes. The results provide a foundation for interpreting rheological measurements, by mechanical and

optical techniques, of dilute suspensions of micron-sized capsules of technological importance.

REFERENCES

BARTHES-BIESEL, D. 1991 Role of interfacial properties on the motion and deformation of capsules in shear flow. *Physica A* **172**, 103–124.

BARTHES-BIESEL, D. & SGAIER, H. 1985 Role of membrane viscosity in the orientation and deformation of a spherical capsule suspended in simple shear flow. *J. Fluid Mech.* **160**, 119–135.

CHANG, K. S. 1991 Experimental study of capsule motion and deformation in linear shear flows. PhD thesis, Cornell University.

CHANG, K. S. & OLBRICHT, W. L. 1993 Experimental studies of the deformation of a synthetic capsule in extensional flow. *J. Fluid Mech.* **250**, 587–608.

FENG, W. W. & YANG, W. H. 1973 On the contact problem of an inflated spherical nonlinear membrane. *Trans. ASME* E: *J. Appl. Mech.* **40**, 209–214.

GOLDSMITH, H. L. & MARLOW, J. 1972 Flow behavior of erythrocytes. I. Rotation and deformation in dilute suspensions. *Proc. R. Soc. Lond.* B **182**, 351–384.

KELLER, S. R. & SKALAK, R. 1982 Motion of a tank-treading ellipsoidal particle in a shear flow. *J. Fluid Mech.* **120**, 27–47.

LARDNER, T. J. & PUJARA, P. 1977 Analysis of deformations of cell membranes. In *Proc. the Biomechanics Symp. Yale Univ., AMP 23 New Haven, Ct*, pp. 65–67.

LARDNER, T. J. & PUJARA, P. 1978 On the contact problem of a highly inflated spherical nonlinear membrane. *Trans. ASME* E: *J. Appl. Mech.* **45**, 202–203.

LARDNER, T. J. & PUJARA, P. 1980 Compression of spherical cells. *Mech. Today* **5**, 161–176.

LI, X. Z., BARTHES-BIESEL, D. & HELMY, A. 1988 Large deformations and burst of a capsule freely suspended in an elongational flow. *J. Fluid Mech.* **187**, 179–196.

RODRIGUEZ, F. 1982 *Principles of Polymer Systems*. McGraw-Hill.

SCHMID-SCHÖNBEIN, H. & WELLS, R. 1969 Fluid drop-like transition of erythrocytes under shear. *Science* **165**, 288–291.